

# A compact dual-band bandpass filter using microstrip meander loop and square loop resonators

Sholeh Jahani Maleki<sup>a)</sup> and Massoud Dousti

Department of Electrical Engineering, Islamic Azad University (IAU), Science and Research Branch, Tehran, Iran

a) [sholeh.jahani@gmail.com](mailto:sholeh.jahani@gmail.com)

**Abstract:** A compact dual-band bandpass filter using loop resonators is proposed in this paper. The filter is designed for resonance frequencies of 1.8 GHz and 2.4 GHz. It is fabricated on RT/Duroid 6010 with  $h = 1.27$  mm and a relative dielectric constant  $\epsilon_r = 10.8$ . This filter has achieved excellent scattering parameters and size reduction of approximately 30% compared to conventional microstrip filters. The measured fractional bandwidths are 1.66% and 3.54% at 1.8 GHz and 2.4 GHz, respectively. The filter is evaluated by simulation and measurement with very good agreement.

**Keywords:** dual-band filter, bandpass filter, loop resonators, perturbation

**Classification:** Microwave and millimeter wave devices, circuits, and systems

## References

- [1] A. Görür, "Description of coupling between degenerate modes of a dual-mode microstrip loop resonator using a novel perturbation arrangement and its dual-mode bandpass filter application," *IEEE Trans. Microw. Theory Tech.*, vol. 52, no. 2, pp. 671–677, Feb. 2004.
- [2] H. Miyake, S. Kitazawa, T. Ishizaki, T. Yamada, and Y. Nagatomi, "A miniaturized monolithic dual band filter using ceramic lamination technique for dual mode portable telephones," *IEEE MTT-S Int. Microw. Symp. Dig.*, vol. 2, pp. 789–792, June 1997.
- [3] I. Wolff, "Microstrip bandpass filter using degenerate modes of a microstrip ring resonator," *Electron. Lett.*, vol. 8, no. 12, June 1972.
- [4] J. X. Chen, T. Y. Yum, J. L. Li, and Q. Xue, "Dual-Mode Dual-Band Bandpass Filter Using Stacked-Loop Structure," *IEEE Microw. Wireless Compon. Lett.*, vol. 16, no. 9, Sept. 2006.
- [5] J. S. Hong and M. J. Lancaster, "Microstrip Bandpass Filter Using Degenerate Modes of a Novel Meander Loop Resonator," *IEEE Microw. Wireless Compon. Lett.*, vol. 5, no. 11, Nov. 1995.

## 1 Introduction

Recently, dual band microstrip filters have an important role in most Microwave and RF applications. Many communication systems such as GSM or WLAN ones operate in dual bands. Many researchers have investigated numerous dual-mode microstrip bandpass filters for applications in wireless communication because of their advantages in applications requiring narrow-band microwave bandpass filters with features such as small size, low loss and low mass [1, 2, 3]. To date, numerous authors have proposed different types of microstrip bandpass filters using the degenerate modes of resonators [3]. The two degenerate modes of a dual-mode resonator to realize a bandpass filter are excited and coupled to each other by adding different forms of perturbations [1]. The strength of the coupling between the degenerate modes of the dual-mode resonator is determined by the perturbation's shape and size.

A compact dual-band bandpass filter using microstrip loop resonators with square patches is presented in this paper. The filter provides two transmission paths to an RF signal, and each of them is realized using loop resonators. The perturbation element is the square patches used in resonators. This Filter requires only single input and output. Compared with the conventional dual band filters, the filter is better in performance and smaller in size.

## 2 Microstrip loop resonators

This paper introduces a compact dual-band Bandpass filter using microstrip meander loop and square loop resonators. The schematic layout of the meander loop resonator is shown in Fig. 1 a, which shows that the meander loop resonator has a compact size. This resonator is designed at 1.8 GHz. An inner corner perturbation is introduced in the resonator. The strength of the coupling between the modes depends on the size of the perturbation element. The designed meander loop resonator has following parameters:  $a = 13$  mm,  $b = 3.17$  mm,  $c = 2$  mm,  $p_1 = 1.6$  mm,  $w_1 = w_3 = 1$  mm,  $w_2 = 0.5$  mm,  $d = 2.8$  mm,  $g = 0.3$  mm and  $w = 1$  mm, which is the width of  $50\ \Omega$  microstrip line.

Fig. 1 b shows layout of a microstrip square loop resonator with an inner perturbation. The square loop resonator has four identical arms in length. The fundamental resonance occurs when  $a \approx \lambda_g/4$ , where  $\lambda_g$  is guided wavelength

$$\lambda_g = \frac{c}{f\sqrt{\varepsilon_{eff}}} \quad (1)$$

Where,  $\varepsilon_{eff}$  is the effective dielectric constant of the substrate, and  $c$  is the velocity of light in free space [4]. According to (1), for a fixed  $\varepsilon_{eff}$ , the resonant frequency  $f$  is decreased as  $a$  increased. Therefore, the fundamental resonant frequency is shifted down. So, to obtain 2.4 GHz, this square loop resonator is designed at 2.67 GHz. It is designed and simulated on a substrate with thickness of 1.27 mm and permittivity of 10.8. The designed loop

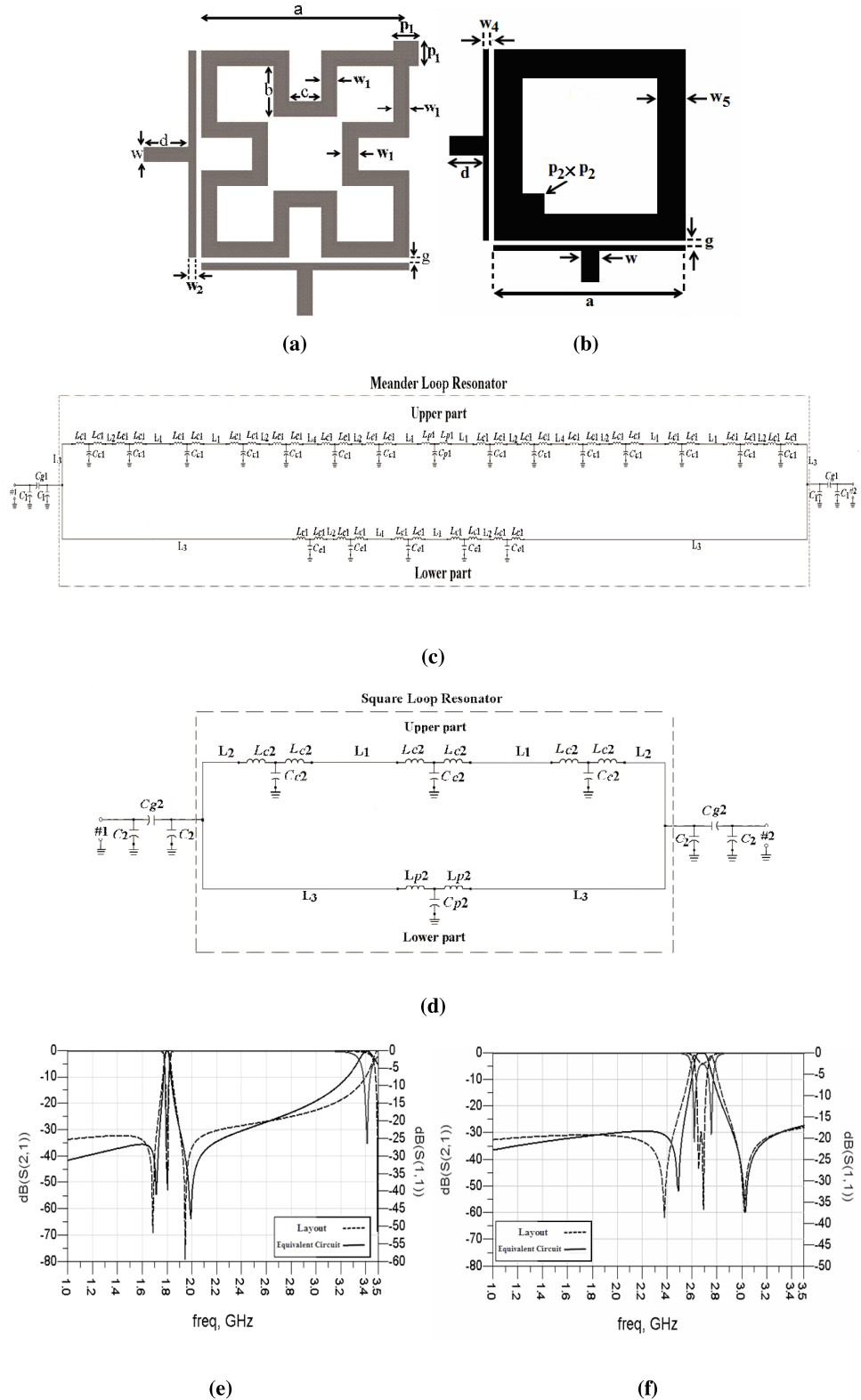


Fig. 1. (a) schematic layout of the meander loop resonator (b) schematic layout of the square loop resonator (c) transmission-line model of the meander loop resonator (d) transmission-line model of the square loop resonator (e) Simulated frequency responses of the meander loop resonator (f) Simulated frequency responses of the square loop resonator

resonator has following parameters:  $a = 13$  mm,  $w_4 = 0.5$  mm,  $w_5 = 2.3$  mm,  $d = 2.8$  mm,  $p_2 = 2.03$  mm,  $g = 0.3$  mm and  $w = 1$  mm, which is the width of  $50\ \Omega$  microstrip line.

The Meander loop and square loop resonators represent shunt circuits, which there are two propagation paths between the input and output ports. Fig. 1 c and Fig. 1 d show the equivalent transmission-line models of the meander loop and square loop resonators configuration. The resonators are symmetrical. The total length of the loop resonators is  $\lambda_g$  at the fundamental resonance frequency. The equivalent capacitances  $C_i$  ( $i = p_1, p_2, c1, c2$ ) and inductances  $L_i$  ( $i = p_1, p_2, c1, c2$ ) of the corner and perturbation elements are given by:

$$\frac{C_i}{W} \left( \frac{pF}{m} \right) = (9.5\epsilon_r + 1.25) \frac{W}{h} + 5.2\epsilon_r + 7.0. \quad (2)$$

$$\frac{L_i}{h} \left( \frac{nH}{m} \right) = 100 \left( 4\sqrt{\frac{W}{h}} - 4.21 \right). \quad (3)$$

Where,  $W$  is the line width of the corner or perturbation elements and  $h$  is the substrate thickness. In the equations (2) and (3), all lengths are in mm. In the equivalent transmission-line models of the loop resonators,  $l_x$  ( $x = 1, \dots, 4$ ) and  $l_s$  ( $s = 1, \dots, 3$ ) are lengths of transmission lines. The capacitances  $C_{g1}$  and  $C_{g2}$  are due to the charge buildup between the two microstrip lines. The capacitances  $C1$  and  $C2$  are due to the fringing fields at the open circuits.

The parameters of the meander loop resonator are shown as follows:  $l_1 = 3.5$  mm,  $l_2 = 2.17$  mm,  $l_3 = 1$  mm and  $l_4 = 2$  mm. The calculated parameters of meander loop resonator are  $C_{c1} = 0.1258$  pF,  $C_{p1} = 0.31$  pF,  $L_{p1} = 0.035$  nH,  $L_{c1} = -0.66$  nH,  $C_1 = 0.592$  pF and  $C_{g1} = 0.636$  pF. A comparison between simulated frequency responses of the loop resonator is shown in Fig. 1 e. It is observed that two transmission poles are realized at 1.64 GHz and 1.94 GHz near the passbands.

The parameters of the square loop resonator are shown as follows:  $l_1 = 8.4$  mm,  $l_2 = 4.2$  mm and  $l_3 = 2.17$  mm. The calculated parameters of square loop resonator are  $C_{c2} = 0.577$  pF,  $C_{p2} = 1.806$  pF,  $L_{p2} = 0.403$  nH,  $L_{c2} = 0.149$  nH,  $C_2 = 0.127$  pF and  $C_{g2} = 0.674$  pF. A comparison between simulated frequency responses of the loop resonators is shown in Fig. 1 f. It is observed that two transmission poles are realized at 2.61 GHz and 2.75 GHz near the passbands.

### 3 Proposed bandpass filter

The 3-D view of proposed dual-band bandpass filter is shown in Fig. 2 a. The bottom side of upper substrate is ground plane. The substrate without ground plane at its bottom side is stacked on the mid-layer loop, which increases the  $\epsilon_{eff}$  effectively. So, the fundamental resonant frequency is shifted down from 2.67 GHz to 2.4 GHz. The two substrates with dielectric constant  $\epsilon_r = 10.8$  and thickness  $h = 1.27$  mm are used for our proposed bandpass

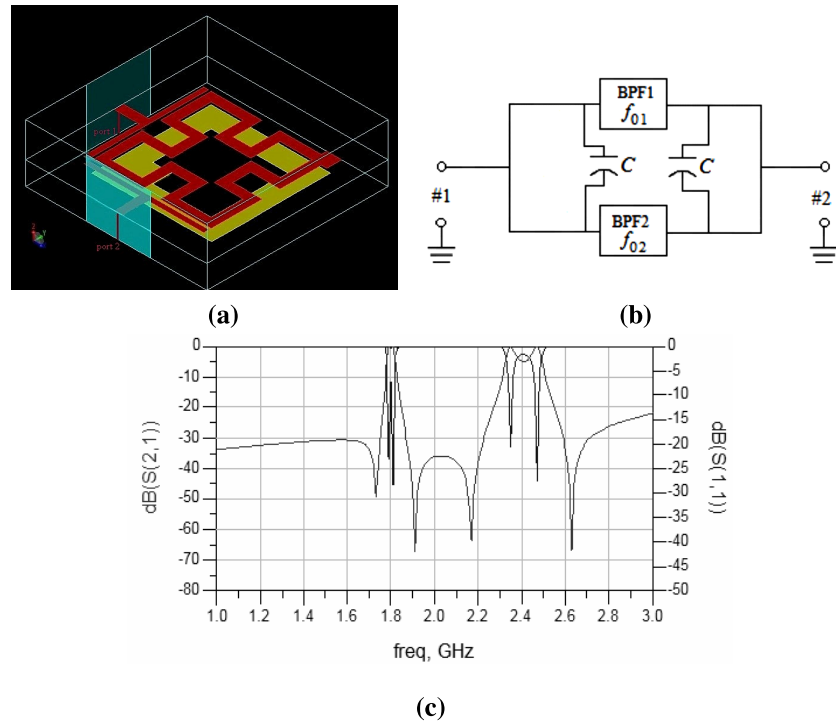


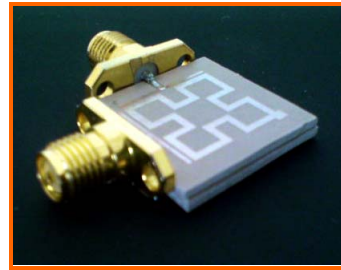
**Fig. 2.** (a) 3-D view of proposed dual-band bandpass filter (b) transmission-line model of the dual-band bandpass filter configuration (c) simulated frequency response of the equivalent transmission-line model

filter design. The two loops located on mid-layer and top-layer provide two transmission paths to RF signal. The proposed filter generates two separated passbands by using two loops resonating different frequency, top-layer loop for lower passband, and mid-layer loop for higher passband. In addition, meander loop and square loop resonators generate own passband and two attenuation poles at respective stopbands.

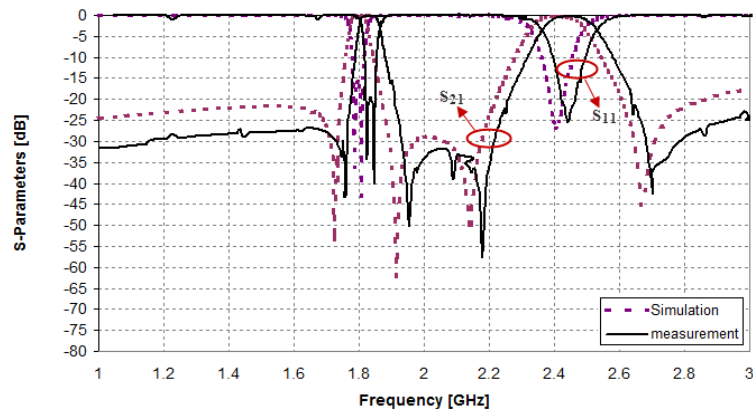
The two patches are attached to different corners of mid-layer loop and top-layer loop for reducing the coupling between the two perturbation patches. This filter needs only single input and output. The dual-band bandpass filter represents a shunt circuit, which there are two propagation paths between the input and output ports. Fig. 2 b shows the equivalent transmission-line model of the Dual-Band bandpass filter configuration. The upper and lower paths are meander loop and square loop resonators, respectively. The capacitance  $C$  is due to coupling between two resonators. Simulated frequency response of the equivalent transmission-line model is shown in Fig. 2 c. Four transmission poles are realized near the passbands.

#### 4 Simulated and measured results

The designed Dual-band bandpass filter was fabricated and measured. A photograph of it is shown in Fig. 3 a. The dual-band BPF is fabricated on two RT/Duroid substrates with dielectric constant 10.8, thickness  $h = 1.27$  mm and  $\tan \delta = 0.0023$ . Dual-band bandpass filter is implemented with a total



(a)



(b)

**Fig. 3.** (a) photograph of the proposed dual-band bandpass filter (b) The simulated and measured performance of the proposed filter

area of  $20 \times 20 \text{ mm}^2$ . The fabricated bandpass is then measured its performance using an Agilent 8722D network analyzer. A comparison between measured and simulated performance of this filter is presented in Fig. 2 b. The simulated 3-dB bandwidths are about 1.51% and 3.5%, while the 3-dB measured bandwidths are 1.66% and 3.54% at the center frequencies of 1.8 GHz and 2.4 GHz, respectively. This compact dual-band bandpass filter is suitable for GSMs and Wireless LAN protocols, such as IEEE 802.11 applications. The minimum insertion losses are 0.18 dB and 0.38 dB higher than the simulated values of 1.8 GHz and 2.4 GHz, respectively. Four transmission poles are realized at 1.75 GHz, 1.95 GHz, 2.18 GHz and 2.7 GHz. The return losses are better than  $-34 \text{ dB}$  and  $-22 \text{ dB}$  at the resonant frequencies of 1.8 GHz and 2.4 GHz, respectively. The compact dual-band bandpass filter has the smallest size with the size reduction of about 30% against the dual-band microstrip loop filters were referred in [4] and [5]. The advantages of the proposed filter are narrower bandwidth, high quality factor, smaller size, and low loss. The good agreements between simulated and measured results validates the proposed filter.

## 5 Conclusion

This paper presents a compact dual-band bandpass filter using meander loop and square loop structures, with the advantages of low loss, narrow bandwidth, high quality factor and compact size. After the explanations of the frequency responses of the resonators, the filter is designed, fabricated and measured. The two loop resonators on different layers generate respective passband. Four attenuation poles are realized near the passbands. This new structure has size reduction of about 30% against the conventional dual-band band-pass filters. The good agreement between simulated and measured results validates the proposed filter.